1686 *Chem. Mater.* **2010,** *22,* 1686–1694
DOI:10.1021/cm903080k

CHEMISTRY OF MATERIALS
Article

Evolution of Metal-Trifluoroacetate Precursors in the Thermal Decomposition toward High-Performance $YBa_2Cu_3O_7$ Superconducting Films

A. Llordés,[†] K. Zalamova,[†] S. Ricart,[†] A. Palau,[†] A. Pomar,[†] T. Puig,[†] A. Hardy,[‡] M. K. Van Bael,[‡] and X. Obradors*,[†]

[†]*Institut de Ciència de Materials de Barcelona, ICMAB-CSIC. Campus de la UAB, 08193 Bellaterra, Catalonia, Spain and* [‡]*Hasselt University, Inorganic and Physical Chemistry Group-Institute for Materials Research, Diepenbeek, Belgium*

Received October 5, 2009. Revised Manuscript Received December 15, 2009

A thorough analytical study on the thermal decomposition evolution of the metal-trifluoroacetate precursor toward high-performance $YBa_2Cu_3O_7$ superconducting films is presented. Evolved gas analysis (EGA), using Fourier transform infrared spectroscopy (FTIR) and mass spectrometry (MS), as well as X-ray diffraction (XRD), was performed to determine the complete chemical decomposition reaction of the metal-trifluoroacetate precursors. It is noteworthy that, contrary to what had been previously described, HF was not detected in the released gas. Moreover, we present new processing conditions that successfully reduced and even eliminated the undesirable porosity of the pyrolyzed films. Focused-ion-beam (FIB) studies demonstrated that the formation of pores was related to a fast escape of the released gas during precursor decomposition. The oxygen partial pressure was determined to be a key parameter to control both the kinetics and thermodynamics of the decomposition reaction and, hence, the porosity. This is of great importance because dense films are required to achieve high critical current densities in $YBa_2Cu_3O_7$ superconducting films.

Introduction

Solution chemistry is becoming a very promising path toward low-cost preparation of functional thin-film materials and nanostructures.[1−8] Many different types of functional oxides (ferromagnetic, superconducting, ferroelectric, etc.) have been prepared,[9−11] displaying performances that are competitive with physical deposition methodologies where high vacuum equipment is required. A key goal for solution-based techniques is to achieve a detailed understanding and control of the four steps involved in the process, together with their mutual interrelationship: (i) precursor chemistry and solution preparation, (ii) solution deposition, (iii) decomposition of the chemical precursors toward an intermediate amorphous and/or nanocrystalline solid, and (iv) nucleation and growth of the final crystalline materials. Previous studies[12−17] demonstrated that a complex relationship exists among the processing parameters, microstructure, and performances. Therefore, a thorough investigation of the mechanisms involved in the microstructural evolution at different steps is required, together with knowledge of its influence on the final performances of the functional materials.

Coated conductors (CCs),[18] which are based on $YBa_2Cu_3O_{7-x}$ (YBCO), are a second generation of high-current conductors that display outstanding performance at

*Author to whom correspondence should be addressed. Tel.: +34935801853. E-mail: obradors@icmab.es.

(1) Hardy, A.; Mondelaers, D.; Vanhoyland, G.; Van Bael, M. K.; Mullens, J.; Van Poucke, L. C. *J. Sol−Gel Sci. Technol.* **2003**, *26*, 1103–1107.
(2) Schwartz, R. W.; Schneller, T.; Waser, R. *C. R. Chim.* **2004**, *7*, 433–461.
(3) Shimoda, T.; Matsuki, Y.; Furusawa, M.; Aoki, T.; Yudasaka, I.; Tanaka, H.; Iwasawa, H.; Wang, D. H.; Miyasaka, M.; Takeuchi, Y. *Nature* **2006**, *440*, 783–786.
(4) Tung, V. C.; Allen, M. J.; Yang, Y.; Kaner, R. B. *Nat. Nanotechnol.* **2009**, *4*, 25–29.
(5) Gibert, M.; Puig, T.; Obradors, X.; Benedetti, A.; Sandiumenge, F.; Huhne, R. *Adv. Mater.* **2007**, *19*, 3937–+.
(6) Zhong, X. L.; Wang, J. B.; Liao, M.; Huang, G. J.; Xie, S. H.; Zhou, Y. C.; Qiao, Y.; He, J. P. *Appl. Phys. Lett.* **2007**, *90*.
(7) Liu, M.; Li, X.; Lou, J.; Zheng, S. J.; Du, K.; Sun, N. X. *J. Appl. Phys.* **2007**, *102*.
(8) Carretero-Genevrier, A.; Mestres, N.; Puig, T.; Hassini, A.; Oro, J.; Pomar, A.; Sandiumenge, F.; Obradors, X.; Ferain, E. *Adv. Mater.* **2008**, *20*, 3672–+.
(9) Gutierrez, J.; Llordes, A.; Gazquez, J.; Gibert, M.; Roma, N.; Ricart, S.; Pomar, A.; Sandiumenge, F.; Mestres, N.; Puig, T.; Obradors, X. *Nat. Mater.* **2007**, *6*, 367–373.
(10) Kim, J. K.; Kim, S. S.; Kim, W. J.; Bhalla, A. S.; Guo, R. *Appl. Phys. Lett.* **2006**, *88*.
(11) Wan, J. G.; Wang, X. W.; Wu, Y. J.; Zeng, M.; Wang, Y.; Jiang, H.; Zhou, W. Q.; Wang, G. H.; Liu, J. M. *Appl. Phys. Lett.* **2005**, *86*.
(12) Hasenkox, U.; Hoffmann, S.; Waser, R. *J. Sol−Gel Sci. Technol.* **1998**, *12*, 67–79.
(13) Levi, C. G. *Acta Mater.* **1998**, *46*, 787–800.
(14) Hardy, A.; Nelis, D.; Vanhoyland, G.; Van Bael, M. K.; Van den Rul, H.; Mullens, J.; Van Poucke, L. C.; D'Haen, J.; Goux, L.; Wouters, D. J. *Thin Solid Films* **2005**, *492*, 105–113.
(15) Iakovlev, S.; Solterbeck, C. H.; Kuhnke, M.; Es-Souni, M. *J. Appl. Phys.* **2005**, *97*.
(16) McIntyre, P. C.; Cima, M. J.; Smith, J. A.; Hallock, R. B.; Siegal, M. P.; Phillips, J. M. *J. Appl. Phys.* **1992**, *71*, 1868–1877.
(17) Puig, T.; Gonzalez, J. C.; Pomar, A.; Mestres, N.; Castano, O.; Coll, M.; Gazquez, J.; Sandiumenge, F.; Pinol, S.; Obradors, X. *Supercond. Sci. Technol.* **2005**, *18*, 1141–1150.
(18) Larbalestier, D.; Gurevich, A.; Feldmann, D. M.; Polyanskii, A. *Nature* **2001**, *414*, 368–377.

Published on Web 01/20/2010

temperatures and magnetic fields much higher than any other known superconducting material. Therefore, they have opened a new avenue for the applications of superconductivity in power systems and magnets. However, to achieve the required performance, an unavoidable hurdle is to develop high-throughput methodologies which, additionally, must be efficient to produce the long-length highly textured multilayered architecture required for such CCs. Chemical solution deposition (CSD) has been demonstrated to be a very promising technique for the large-scale production of CCs and, hence, a wide effort for detailed understanding of the mechanisms involved in the preparation of the complex CC architecture is being performed.[19,20]

In particular, the metal-organic decomposition (MOD) of trifluoroacetate (TFA) precursor solutions has attracted much interest since its early discovery by Gupta et al.[21] and YBCO films with similar performance to the vacuum-deposited ones were promptly achieved.[22] The interest of fluorinated precursors lies in the formation of BaF_2 as an intermediate nanostructured phase, instead of $BaCO_3$, which has a higher decomposition temperature. Moreover, further BaF_2 decomposition is determined by the water content in the gas flow, making possible, then, a fine tuning of the film growth rate through the water pressure parameter. Many detailed investigations on the use of these metal-organic precursors have been reported,[23,24] including recent developments of modified TFA solutions, which enable the in situ growth of superconducting nanocomposite thin films with improved performances.[9,25−29]

Despite the wide use of the TFA precursors in the preparation of YBCO films, a detailed understanding of the mechanisms that control the chemical precursor conversion to the final highly textured films is still far from being achieved. The decomposition step of the MOD process for YBCO growth, i.e., the pyrolysis process, was initially limiting the overall yield of the conductor production, because of the very long duration (~24 h) required to maintain film homogeneity. Further investigation of the stress relief mechanisms during the decomposition of anhydrous TFA precursors showed that much shorter processes could be used (~0.5 h).[30] Shortening the pyrolysis time requires an accurate selection of the processing parameters that control the shrinkage process and the diffusion of exhaust gas. The poor mechanical properties of the gellified film may easily lead to the formation of defects and inhomogeneities such as cracks, blisters, or film buckling, each having strong influence on the final quality of the pyrolyzed and subsequent grown films.[30] Some controversy exists, however, concerning the relevance of different parameters on the film degradation process. It has been suggested that reducing the fluorine content in the metal-organic precursors could help to lessen inhomogeneities in the resulting film (e.g., blistering,[31] surface damages generated by bubbling,[32] etc.) due to the fluorinated released gases. These issues were even more critical in multideposition,[33] where intermediate deposition−pyrolysis processes were added to fabricate films with larger thickness. In that case, phase separation at the interfaces was very often observed showing detrimental effects on the film performance. Therefore, it is clear that a crucial point in the MOD process toward YBCO films preparation is the precursor decomposition chemical reaction. Furthermore, the identification of the released gases during TFA decomposition could sort out its possible nuisance on the final film homogeneity, microstructure, and physical properties, as well as its potentially harmful environmental effects and toxicity.

The decomposition reaction of metal trifluoroacetates has been described by several authors with different degrees of detail.[23,34,35] This reaction is essentially described by Scheme 1. Surprisingly, however, the chemical reaction that occurs in Scheme 1 is poorly understood and the unknown gaseous phases have been essentially assigned[23,34] to CO, CO_2, HF, and C_nF_{2n+2}.

In this work, we present a thorough analytical study of both gaseous and solid decomposition products of the TFA precursor gel, as well as the influence of the gas flow atmosphere in such products. EGA was performed either by thermogravimetric analysis−Fourier transform infrared analysis (TGA-FTIR) and thermogravimetric analysis−mass spectroscopy (TGA-MS). X-ray diffraction

(19) Izumi, T.; Yoshizumi, M.; Miura, M.; Sutoh, Y.; Nakanishi, T.; Nakai, A.; Ichikawa, Y.; Yamada, Y.; Goto, T.; Yajima, A.; Aoki, Y.; Hasegawa, T.; Shiohara, Y. *Physica C* **2008**, *468*, 1527–1530.
(20) Obradors, X.; Puig, T.; Pomar, A.; Sandiumenge, F.; Mestres, N.; Coll, M.; Cavallaro, A.; Roma, N.; Gazquez, J.; Gonzalez, J. C.; Castano, O.; Gutierrez, J.; Palau, A.; Zalamova, K.; Morlens, S.; Hassini, A.; Gibert, M.; Ricart, S.; Moreto, J. M.; Pinol, S.; Isfort, D.; Bock, J. *Supercond. Sci. Technol.* **2006**, *19*, S13–S26.
(21) Gupta, A.; Jagannathan, R.; Cooper, E. I.; Giess, E. A.; Landman, J. I.; Hussey, B. W. *Appl. Phys. Lett.* **1988**, *52*, 2077–2079.
(22) McIntyre, P. C.; Cima, M. J.; Ng, M. F. *J. Appl. Phys.* **1990**, *1*, 4183–4187.
(23) Rupich, M. W.; Verebelyi, D. T.; Zhang, W.; Kodenkandath, T.; Li, X. P. *MRS Bull.* **2004**, *29*, 572–578.
(24) Wesolowski, D. E.; Yoshizumi, M.; Cima, M. J. *IEEE Trans. Appl. Supercond.* **2007**, *17*, 3351–3354.
(25) Goswami, R.; Holtz, R. L.; Rupich, M. W.; Zhang, W.; Spanos, G. *Acta Mater.* **2007**, *55*, 6746–6753.
(26) Cui, X. M.; Tao, B. W.; Tian, Z.; Xiong, J.; Zhang, X. F.; Li, Y. R. *Supercond. Sci. Technol.* **2006**, *19*, 844–847.
(27) Arenal, R.; Miller, D. J.; Maroni, V. A.; Rupich, M. W.; Li, X.; Huang, Y.; Kodenkandath, T.; Civale, L.; Maiorov, B.; Holesinger, T. G. *IEEE Trans. Appl. Supercond.* **2007**, *17*, 3359–3362.
(28) Holesinger, T. G.; Civale, L.; Maiorov, B.; Feldmann, D. M.; Coulter, J. Y.; Miller, J.; Maroni, V. A.; Chen, Z. J.; Larbalestier, D. C.; Feenstra, R.; Li, X. P.; Huang, M. B.; Kodenkandath, T.; Zhang, W.; Rupich, M. W.; Malozemoff, A. P. *Adv. Mater.* **2008**, *20*, 391–407.
(29) Engel, S.; Thersleff, T.; Huhne, R.; Schultz, L.; Holzapfel, B. *Appl. Phys. Lett.* **2007**, *90*.
(30) Zalamova, K.; Roma, N.; Pomar, A.; Morlens, S.; Puig, T.; Gazquez, J.; Carrillo, A. E.; Sandiumenge, F.; Ricart, S.; Mestres, N.; Obradors, X. *Chem. Mater.* **2006**, *18*, 5897–5906.
(31) Tokunaga, Y.; Honjo, T.; Izumi, T.; Shiohara, Y.; Iijima, Y.; Saitoh, T.; Goto, T.; Yoshinaka, A.; Yajima, A. *Cryogenics* **2004**, *44*, 817–822.
(32) Siegal, M. P.; D., J. T.; Overmyer, D. L. *J. Mater. Res.* **2001**, *16*, 3339–3342.
(33) Nakaoka, K.; Tokunaga, Y.; Matsuda, J. S.; Fuji, H.; Koyama, S.; Teranishi, R.; Izumi, T.; Shiohara, Y.; Watanabe, T.; Yamada, Y.; Goto, T.; Yoshinaka, A.; Yajima, A. *Physica C* **2005**, *426−431*, 954–958.
(34) Araki, T.; Hirabayashi, I. *Supercond. Sci. Technol.* **2003**, *16*, R71–R94.
(35) Gazquez, J.; Sandiumenge, F.; Coll, M.; Pomar, A.; Mestres, N.; Puig, T.; Obradors, X.; Kihn, Y.; Casanove, M. J.; Ballesteros, C. *Chem. Mater.* **2006**, *18*, 6211–6219.

Scheme 1. Decomposition Reaction of the Metal-Trifluoroacetate Precursors

$$Y(CF_3COO)_3 + 2Ba(CF_3COO)_2 + 3Cu\,(CF_3COO)_2 \rightarrow CuO + Ba_{2-x}Y_xF_{2+x} + \text{gaseous phases}$$

(XRD) of the resulting solid product after the thermal treatment has also been performed. This study has allowed us to define, for the first time, a complete decomposition reaction where the gaseous phases indicated in Scheme 1 have been identified. Particularly, contrary to what is widely believed, no hydrofluoric acid (HF) was detected during the pyrolysis step, which is a key point to assess the degree of chemical toxicity of the exhaust.

Porosity development in the as-decomposed films has also been investigated through cross-sectional focused-ion-beam (FIB) images. It is well-known[36,37] that the residual porosity in YBCO films has strong influence with regard to decreasing the critical current density (J_c), because the pores behave as current blocking defects. Feenstra et al.[38] proposed a densification step based on an intermediate high-temperature annealing. However, this process was accompanied by the formation of a liquid phase, which has detrimental effects, from the viewpoint of compositional and structural control.

In the present work, we show the first results where new conditions are observed to modify the precursor decomposition path, resulting in a key factor to control and eliminate the porosity in these materials. Therefore, fine tuning of the pyrolysis process may be achieved to keep an optimal microstructure and homogeneity of the pyrolyzed films at high decomposition rates.

Experimental Section

Synthesis of the Precursor Solution. Yttrium, barium, and copper trifluoroacetate (TFA) salts were prepared by reaction from commercial YBCO powder ($YBa_2Cu_3O_x$, Solvay) with an excess of trifluoroacetic anhydride (Aldrich, 99%) and a small quantity of trifluoroacetic acid (Aldrich, 99%) as a catalyst. Freshly distilled acetone (Panreac PA) was used as a solvent. After stirring the mixture for 72 h at 50 °C and evaporating the solvents under vacuum, a mixture of TFA salts ($Y(TFA)_3$, $Ba(TFA)_2$, and $Cu(TFA)_3$) in a stoichiometric ratio of 1:2:3 was obtained.[39] The final total metal ion concentration of 1.5 M was obtained by adding anhydrous methyl alcohol.

YBCO Thin-Film Preparation. Solution deposition on $LaAlO_3$ or $SrTiO_3$ (100)-oriented single crystal substrate was performed by spin coating. Further details of the deposition have been described elsewhere.[39] A pyrolysis step was performed in a tubular furnace under an oxygen gas flow (50 mL/min). Nitrogen and air gas-flow atmospheres have also been used to study its influence in the decomposition kinetics. The following heating profiles were used: 5 °C/min up to 250 °C, 3 °C/min up to 300 °C, and a variable time at 300 °C, depending on the gas atmosphere (30 min with O_2 and 60 min with N_2 and air). The crystallization step was performed for 150 min at a reacting temperature of 810−830 °C in a wet N_2 atmosphere with water vapor partial pressure ($P(H_2O)$) of 22 mbar and an O_2 partial pressure of 0.2 mbar. Finally, the superconducting phase was achieved by oxygen annealing at 450 °C.

Characterization Techniques. The thermal decomposition pathway of TFA precursor solution was examined by means of thermogravimetric analysis (TGA) (TA Instruments TGA 951-2000) online coupled to a FTIR spectrometer (Bruker IFS 66, resolution = 4 cm^{-1}) or a quadrupole mass spectrometer (MS, Thermolab VG Fisons). Both of these techniques permit the analysis of the gases emitted during decomposition; however, here, they are used in a complementary manner.[40] The identification of gas molecules becomes easier with FTIR, because no fragmentation occurs; however, a lower detection limit is achieved with MS. The evolved gases were identified based on their FTIR and MS reference spectra, which are available in the public domain spectrum libraries of NIST[41] and SBDS.[42]

TGA-MS measurements were performed at an ionization energy of 70 eV and scans have been performed in the range between $m/z = 10$ and $m/z = 120$, because the most important ions were expected to be situated here. To evaporate the solvent (MeOH) from solution, a dwell step of 60 min at 70 °C was applied prior to the standard decomposition thermal profile.

All TGA-MS and TGA-FTIR analysis were performed using a dynamic atmosphere of dry or humid synthetic air (50 mL/min). The decomposition solid residues and the pyrolyzed films were analyzed by XRD (using a Bruker AXS D8 Advanced GADDS diffractometer equipped with an area detector). Chemical analysis of the solid deposit at the furnace tube was performed by means of inductively coupled plasma−atomic emission spectroscopy (ICP-AES) on a Perkin−Elmer Optima 3000 DV.

Cross-sectional images were obtained using a dual-beam scanning electron microscopy/focused-ion-beam (SEM, FIB) system (Zeiss, Model 1560 XB). Film thickness was determined either by surface profilometry or from FIB images, and they were in the range of 250−275 nm. The critical current density of the films, at self-field, was determined from inductive measurements performed with a SQUID magnetometer and calculated

(36) Pomar, A.; Gutierrez, J.; Palau, A.; Puig, T.; Obradors, X. *Phys. Rev. B* **2006**, *73*.
(37) Bartolomé, E.; Gömory, F.; Granados, X.; Puig, T.; Obradors, X. *Supercond. Sci. Technol.* **2007**, *20*, 895–899.
(38) Feenstra, R.; Miller, D. Presented at the Superconductivity for Electric Systems Annual Peer Review, Arlington, VA, July 29−31, 2008.
(39) Roma, N.; Morlens, S.; Ricart, S. M.; Zalamova, K.; Moreto, J. M.; Pomar, A.; Puig, T.; Obradors, X. *Supercond. Sci. Technol.* **2006**, *19*, 521–527.
(40) Mullens, J. *Handbook of Thermal Analysis and Calorimetry*, Vol. 1; Elsevier: Amsterdam, 1998; pp 509−546.
(41) *NIST Chemistry Webbook*, http://webbook.nist.gov/chemistry/ (accessed December 2008).
(42) Spectral Data Base System for Organic Compounds, http://riodb01.ibase.aist.go.jp/sdbs/cgi-bin/cre_index.cgi?lang=eng/ (accessed December 2008).

Table 1. Chemical Processes and Detected Gaseous Phases Associated with Each Temperature Region in TFA Precursor Gel ($Y(TFA)_3 + Ba(TFA)_2 + Cu(TFA)_2$) Pyrolysis Performed in Synthetic Air

stage	temperature, T (°C)	mass loss (%)	chemical process	detected gaseous phases
I	RT−70	8.88	uncoordinated solvents evaporation	water (H_2O), methanol (CH_3OH), acetone (CH_3COCH_3), trifluoroacetic acid (CF_3COOH)
II	70−240	18.6	coordinated solvents thermolysis and evaporation	methanol (CH_3OH), acetone (CH_3COCH_3), trifluoroacetic acid (CF_3COOH), methyl trifluoroacetate (CF_3COOCH_3)
III	240−300	38.7	thermo-oxidative TFA decomposition	trifluoroacetic acid (CF_3COOH), trifluoroacetyl fluoride (CF_3COF), carbonyl fluoride (COF_2), carbon dioxide (CO_2), carbon monoxide (CO)

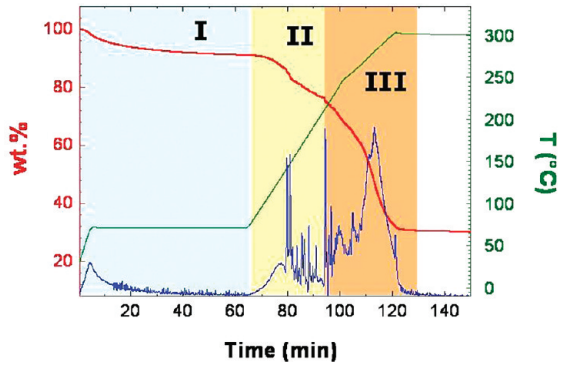

Figure 1. Thermogravimetric analysis (TGA) of the TFA precursor gel in dynamic air. Three main regions exist, according to the weight loss derivative curve (in blue): regions I and II correspond, respectively, to uncoordinated and coordinated solvent evaporation, while region III is related to metal-organic decomposition.

accordingly with the Bean model.[43] We have used the equation $J_c = 3\Delta m/(a^3 t)$,[44] which is valid for squared films, where Δm is the width of the magnetic hysteresis loop at zero field, a the lateral sample dimension (a = 0.5 mm), and t the film thickness.

Results and Discussion

Thermogravimetry and Evolved Gas Analysis. TGA, together with EGA, reveal that the decomposition proceeds in three stages (see Figure 1). The first stage (stage I, $T < 70$ °C) involves both dehydration and evaporation of organic solvents; then, at higher temperatures (T = 70−240 °C), the second stage (stage II)—the thermolysis of coordinated solvents—occurs. Finally, the thermo-oxidative decomposition of TFAs comprises the third stage (stage III, T = 240−300 °C). The chemical processes and the associated released gases (as detected by MS and infrared (IR) analyses) are indicated in Table 1, and they will be described next in more detail.

Stage I: From Room Temperature up to 70 °C. Within this temperature range, the gases detected by MS and FTIR were water (m/z = 18), trifluoroacetic acid (m/z = 114, m/z = 45, carbonyl absorption band at 1830 cm^{-1}), methanol (m/z = 29, m/z = 31), and acetone (m/z = 58, m/z = 43) (see Figure 2a and Table 1). The presence of water is due to the high hygroscopic character of TFA salts, whereas the remaining released gases correspond to residual volatile solvents (bp < 73 °C) coming from the synthesis of the TFA salts solution.

Stage II: T = 70−240 °C. Methanol, trifluoroacetic acid, and acetone were still released within this intermediate thermal region (see Figures 2a and 3). Taking into account that the temperature range is higher than the corresponding boiling points of each compound, their detection can be taken into account by the thermolysis and consequent evaporation, which indicate that such solvents are coordinated.[45] As an example, in Figure 2a, the acetone molecular ion $[CH_3COCH_3]^+$ is detected at approximately its boiling point (57 °C) and it is again observed at temperatures that are much higher, denoting coordination to a metallic center.

It is well-known that an electron-donor heteroatom easily coordinates with a metallic electron-acceptor center in metal-organic systems. In particular, copper and yttrium complexes coordinated to methanol or acetone have been already described.[46] This finding agrees with previous unproved assessments for the existence of coordinated solvents in TFA metal-organic precursors.[47]

The presence of a certain amount of methyl trifluoroacetate, which had not been previously reported (see Figure 3a) is justified by the high reactivity of methanol and trifluoroacetic acid at these temperatures, giving the esterification product as a result.

Stage III: T = 240−300 °C. The detection of $[CF_3]^+$ and $[CO_2]^+$ fragments by MS within the temperature range of 240−300 °C (see Figures 2b and 2c), together with the highest weight loss observed in the TGA (38.7%), are evidence of the thermo-oxidative decomposition of the organic matter. This temperature region was previously identified as being where strong film shrinkage (64% of the film thickness) occurs and, thus, tensile stress relaxation can lead to highly inhomogeneous or even cracked films.[30] For this reason, a tight control of processing parameters within this stage is crucial to get homogeneous and smooth films after pyrolysis.

The gases that evolved during the TFA decomposition in this stage were identified as CF_3COOH, CF_3COF, COF_2, CO_2, and CO (see Figures 2c, 2d, and 3b). Further details about their characterization will be given later in this paper.

Here, we would like to emphasize that no HF signal was detected via either MS or FTIR. The same result was previously reported for the conversion of alkaline-earth and rare-earth TFAs into metal fluoride thin films

(43) Bean, C. P. *Phys. Rev. Lett.* **1962**, *8*, 250.
(44) Chen, D. X.; Goldfarb, R. B. *J. Appl. Phys.* **1989**, *66*, 2489–2500.
(45) Zhang, H. Y.; Hubert-Pfalzgraf, L. G.; Luneau, D. *Polyhedron* **2005**, *24*, 1185–1195.
(46) Mishra, S. *Coord. Chem. Rev.* **2008**, *252*, 1996–2025.
(47) Araki, T.; Hirabayashi, I. *Supercond. Sci. Technol.* **2003**, *16*, R71–R94.

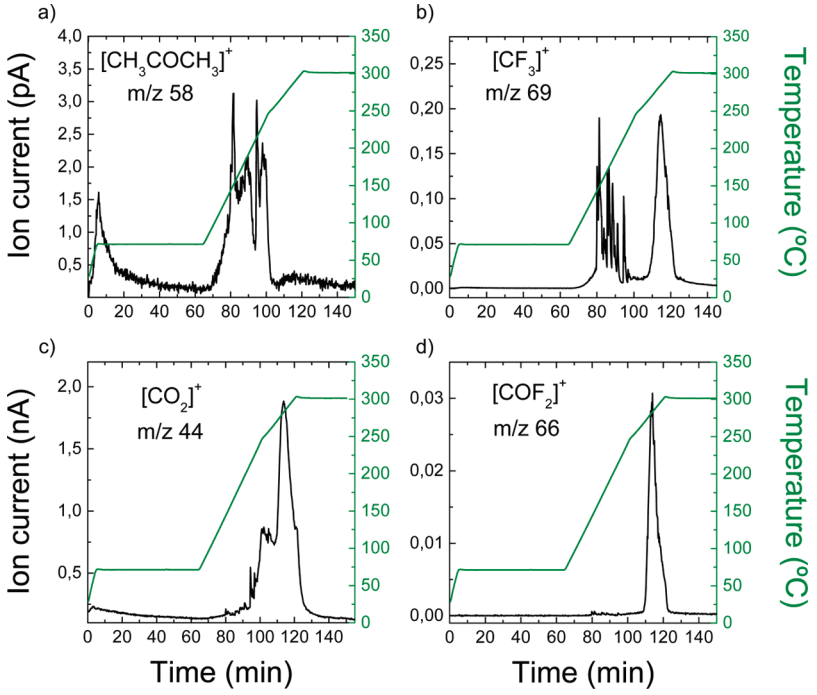

Figure 2. Occurrences of ion mass fragments of the evolved gases, as a function of time, measured with TGA-MS for the TFA precursor decomposition in air: (a) acetone molecular ion ($[CH_3COCH_3]^+$), (b) $[CF_3]^+$ ion fragment, (c) carbon dioxide molecular ion (CO_2^+), and (d) carbonyl fluoride molecular ion (COF_2^+).

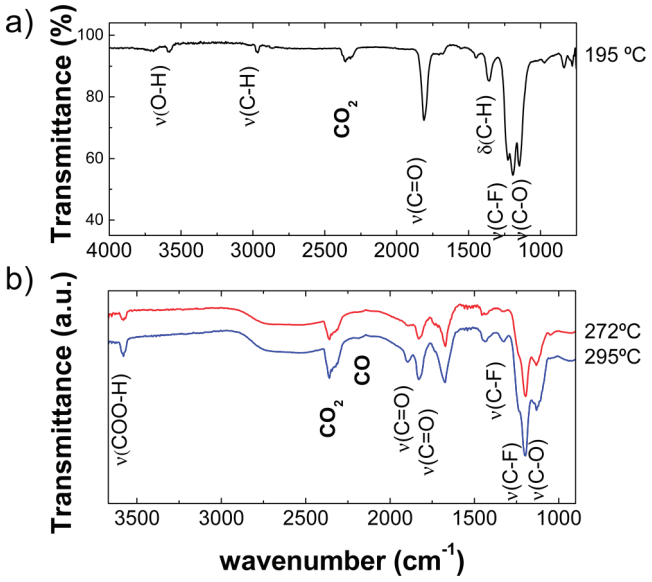

Figure 3. FTIR spectra of the released gases detected at different temperatures during TFA precursors decomposition: (a) at 195 °C, the assigned absorption bands correspond to methyl trifluoroacetate, methanol, and carbon dioxide and (b) between 272 °C and 295 °C, the assigned absorption bands correspond to trifluoroacetic acid, trifluoroacetyl fluoride, carbon dioxide, and carbon monoxide.

for optical applications.[48] Therefore, our results do not support previous, poorly described analysis, which proposed the formation of HF as an exhaust gas in the pyrolysis stage.[31,49] Taking into account that the commonly used electrode for the identification of fluorinated compounds is selective for fluoride ions,[50,51] it is very likely that HF was erroneously identified as a fluoride-containing molecule overlooking the presence of other fluorinated gases such as CF_3COF and COF_2.

FTIR spectra of the gaseous phases released during TFA decomposition at different temperatures are shown in Figure 3. Between 195 and 295 °C, the IR absorption bands at 3580, 1830, and 1200 cm^{-1} are assigned to COO−H, C═O, and C−F stretching vibrations, which correspond to trifluoroacetic acid (TFAH). On the other hand, no absorption band due to trifluoroacetic anhydride (two intense bands should appear at 1870−1725 cm^{-1} due to C═O stretching) has been observed. Trifluoroacetic anhydride (TFAA) easily hydrolyzes to form TFAH, even with moisture from the air; thus, its atmospheric lifetime is believed to be negligible.[52] Taking into account that the pyrolysis process occurs in a humid atmosphere, it is very likely that TFAH is formed due to TFAA hydrolysis. Nevertheless, TFAA was also not detected in a dry atmosphere, thus indicating that a certain amount of water must be present in the gas flow. This is consistent with the detection of the water ion mass (m/z = 18) at temperatures of > 100 °C (see Figure 4), as a result of the esterification reaction, which occurs within temperature region II (between 145 °C and 240 °C).

At higher temperatures (272−295 °C), a new absorption band at 1896 cm^{-1} appears in the IR spectra

(48) Fujihara, S.; Tada, M.; Kimura, T. *J. Sol−Gel Sci. Technol.* **2000**, *19*, 311–314.
(49) Yoo, J.; Kim, Y. K.; Chung, K.; Ko, J.; Wang, X. L.; Dou, S. X. *IEEE Trans. Appl. Supercond.* **2007**, *17*, 3336–3339.
(50) Pinol, S.; Castano, O. *Physica C* **2006**, *450*, 48–55.
(51) Araki, T.; Takahashi, Y.; Yamagiwa, K.; Yuasa, T.; Iijima, Y.; Takeda, K.; Kim, S. B.; Yamada, Y.; Hirabayashi, I. *IEEE Trans. Appl. Supercond.* **2001**, *11*, 2869–2872.
(52) Pruette, L. C.; Karecki, S. M.; Reif, R.; Langan, J. G.; Rogers, S. A.; Ciotti, R. J.; Felker, B. S. *J. Vac. Sci. Technol., A* **1998**, *16*, 1577–1581.

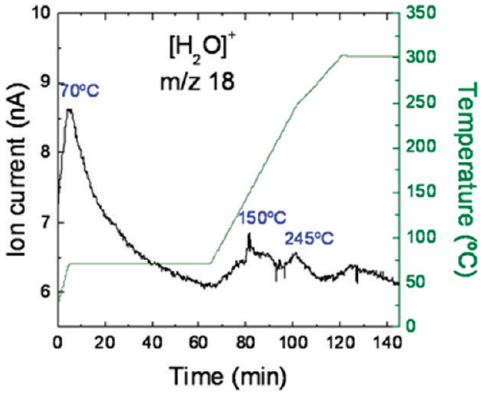

Figure 4. Water ion mass occurrence, as a function of time, measured with TGA-MS for the TFA precursor decomposition under a dry air atmosphere. Water detection at temperatures of >100 °C can be justified by its generation in the esterification reaction between methanol and trifluoroacetic acid.

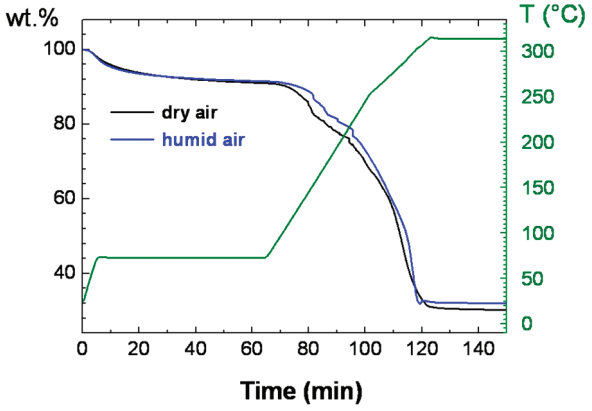

Figure 5. Thermogravimetric analysis of the (Y,Ba,Cu)-TFA precursors showing 4% additional weight loss, under dry conditions.

(see Figure 3b), which is assigned to C=O stretching of CF_3COF.[41] In addition, the COF_2 molecular ion mass was detected by MS within the above-mentioned temperature range (see Figure 2d).

Since TFAH is the first fluorinated compound coming from the decomposition of the TFA moiety, we propose that carbonyl fluoride (COF_2) and trifluoroacetyl fluoride (CF_3COF) may result from further thermo-oxidative decomposition of TFAH, giving CO_2 and CO as decomposition subproducts. The detection of these fluorinated compounds is consistent with previous results described in the literature for the decomposition of TFAH and metal trifluoroacetates.[48,53]

Although TFAH and HF are both acids (pK_a = 0.5 and 3, respectively), their toxicity is completely different. HF is physiologically a very powerful chemical, because F^- ions can bind to Ca^{2+} and Mg^{2+} ions in human tissue by simple exposure.[54] In contrast, TFAH is a stable ion in the aqueous phase and no significant F^- loss process such as hydrolysis, or photolysis, is identified in air. The other fluorinated compounds detected will be mainly toxic, because of the possible formation of HF in their further hydrolysis.[55]

As a conclusion, we state that the released gases during the decomposition of metal trifluoroacetate precursors present much lower toxicity than early believed,[31,34] because no HF is detected. Moreover, taking into account the high reactivity of HF toward SiO_2, its absence in the gas exhaust is also advantageous for the production of large-scale coated conductors, from a technical viewpoint.

Cu Loss due to $Cu(TFA)_2$ Sublimation. It is well-known that the high volatility of copper trifluoroacetate ($Cu(TFA)_2$) causes its partial sublimation at temperatures of >100 °C; thus, some processing modifications had been studied to prevent the loss of copper. McIntryre et al. proposed the addition of water vapor to the gas flow to prevent $Cu(TFA)_2$ sublimation via its hydrostabilization.[56] More recently, diethanolamine (DEA) added to the precursor solution provided similar results.[57] However, no detailed study had been accomplished to analyze and quantify the process, leading to Cu deficiency in the final YBCO superconducting film.

We have studied the sublimation of $Cu(TFA)_2$ through TGA experiments under both dry and humid conditions. When the (Y,Ba,Cu)-TFA precursors decomposed in a dry atmosphere, a solid residue appeared, deposited on the tubular furnace tube. Analysis of the residue by inductively coupled plasma confirmed that it contained copper. The amount of $Cu(TFA)_2$ that sublimated has been quantified by the difference of weight loss observed in the TGA curves. In dry air, the sublimation of $Cu(TFA)_2$ led to an additional weight loss of ~4%, which corresponds to an ~9% Cu deficiency in the $YBa_2Cu_3O_7$ final unit formula. (See Figure 5.) Earlier, Dawley et al.[58] found that YBCO film performance grown under dry conditions was optimized when an excess of 7.5−9% Cu was added to the precursor solution, which is consistent with the copper deficiency that we have determined.

Influence of Gas Atmosphere in the Solid Phases. The role of the oxygen partial pressure is important in coated conductors processing, because unfavorable oxidation of the metallic substrate may occur. Moreover, the oxidizing power of the gas flow during pyrolysis may affect the thermo-oxidative decomposition kinetics, as well as the solid deposit composition.

Previous transmission electron microscopy (TEM) studies determined that the oxygen-decomposed films were a mixture of amorphous regions, intermediate nanocrystalline phases, and porosity.[35] Two-dimensional XRD

(53) Kralj, B.; Zigon, D.; Susic, R. *Rapid Commun. Mass Spectrom.* **1998**, *12*, 87–93.
(54) Alexeeff, G. V.; Lewis, D. C.; Ragle, N. L. *Risk Anal.* **1993**, *13*, 63–69.
(55) Boutonnet, J. C.; Bingham, P.; Calamari, D.; de Rooij, C.; Franklin, J.; Kawano, T.; Libre, J. M.; McCulloch, A.; Malinverno, G.; Odom, J. M.; Rusch, G. M.; Smythe, K.; Sobolev, I.; Thompson, R.; Tiedje, J. M. *Hum. Ecol. Risk Assess.* **1999**, *5*, 59–124.
(56) McIntyre, P. C.; Chiu, R. C.; Cima, M. J.; Rhine, W. E. In *High-Temperature Superconductors: Fundamental Properties and Novel Materials Processing*; Materials Research Society Symposium Proceedings, Vol. *169*, Boston, MA, 1990; pp 743−746.
(57) Dawley, J. T.; Clem, P. G.; Boyle, T. J.; Ottley, L. M.; Overmyer, D. L.; Siegal, M. P. *Physica C* **2004**, *402*, 143–151.
(58) Dawley, J. T.; Clem, P. G.; Siegal, M. P.; Overmyer, D. L.; Rodriguez, M. A. *IEEE Trans. Appl. Supercond.* **2001**, *11*, 2873–2876.

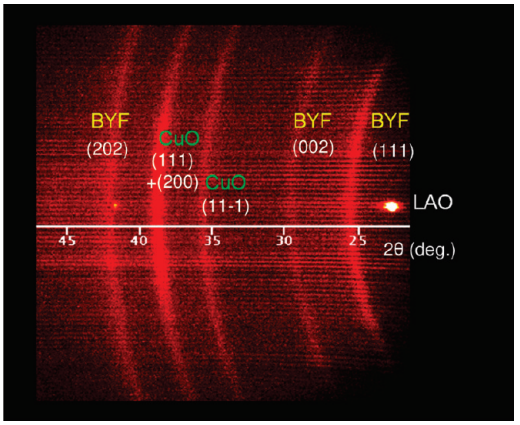

Figure 6. Two-dimensional XRD pattern of a pyrolyzed 500-nm-thick film under standard heating conditions and oxygen gas flow atmosphere. Diffraction cones show the polycrystalline nature of the resultant phases after decomposition, although some preferred orientation is observed. Spots originate from the single-crystal $LaAlO_3$ (LAO) substrate.

of decomposed films proves the polycrystalline nature of the intermediate phases (see Figure 6), which, in an oxygen atmosphere, have been identified as CuO and a $Ba_{0.72}Y_{0.28}F_{2.28}$ (BYF) solid solution.[21,35] However, we note that the intensity of the CuO (111) + (200) Bragg peaks is not uniformly distributed along the diffraction ring, denoting some preferred orientation of the nanocrystallites. Moreover, the BYF solid solution shows a textured component around the [111] direction, in agreement with previous observations.[35] The Y content in the fluoride solid solution was determined from the measured lattice parameter, following a procedure previously reported.[59]

Although BYF crystallizes independently of the oxygen partial pressure, the Cu oxidation state in the oxide phase is strongly affected. A highly oxidizing atmosphere accelerates the thermo-oxidative decomposition reaction, leading to copper(II) oxide (CuO), while the reduced form (Cu_2O) was obtained in an inert N_2 atmosphere. Finally, a mixture of both copper oxide phases was observed in air (see Figure 7a). In addition, the FTIR analysis of the carboxylate group evolution indicates that TFA decomposition is slowed at reduced oxygen partial pressures (see Figure 7b).

In conclusion, and considering the results of the analyses of gaseous and solid phases in an air atmosphere, we propose the chemical reaction in Scheme 2.

The y coefficient in Scheme 2 is related to the Cu_2O fraction formed by reducing the oxygen partial pressure in the gas flow. An increase of CO ($0.5y$ mol) is related to the equivalent formation of Cu_2O, which is a metastable phase in air at this temperature. Therefore, it is very likely that the proposed decomposition reaction (Scheme 2) is valid under inert, reducing, or oxidizing atmospheres if we take into account that the CuO/Cu_2O ratio is modified with PO_2.

Influence of Gas Atmosphere in Film Surface Morphology and Porosity Tuning. A general feature of the chemically

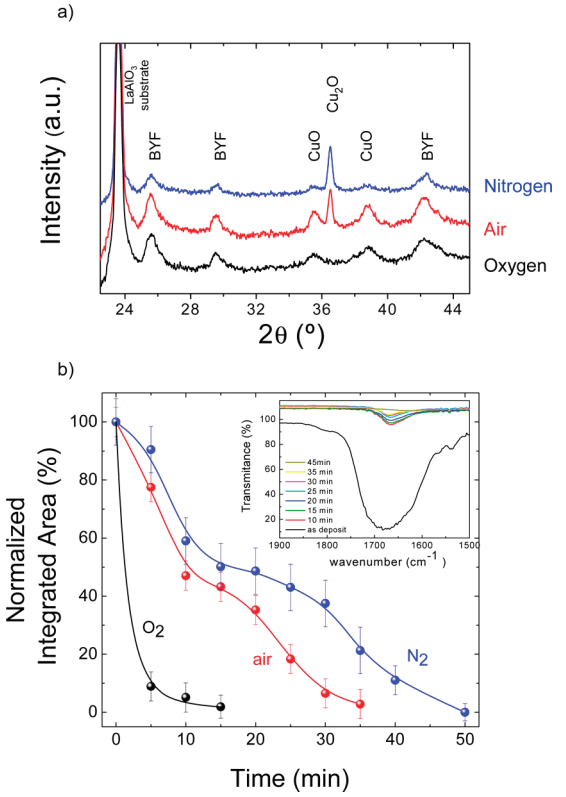

Figure 7. (a) XRD patterns of films pyrolyzed in N_2, air, and O_2. (b) FTIR analysis of the carboxylate evolution during pyrolysis under different atmospheres. The reaction times needed for the complete TFA decomposition are 50 min in N_2, 35 min in air, and 15 min in O_2.

derived films is that a large fraction of precursor volume is eliminated during pyrolysis, hence leading to highly porous films.[2,60] Therefore, porosity has been essentially related to film shrinkage. Moreover, blistering and internal stress relaxation may strongly affect thin-film integrity, which can have detrimental effects on further film crystallization.

It has been recently shown[30] that, through control of several processing parameters during TFA pyrolysis (temperature, gas flow, and heating rate), the stress relief became smoother and homogeneous pyrolyzed films could be achieved. However, the high degree of porosity is still an issue that, until now, has remained unsolved. Residual pores in YBCO films are undesirable because they behave as current blocking defects, thus reducing the percolating J_c value.

We have analyzed the decomposed films through SEM and FIB analyses, to assess whether the different decomposition paths have any influence on the structure and surface morphology.

Figure 8 displays SEM images of as-decomposed films in pure oxygen (P_{Total} = 1 atm), air (P_{O_2} = 0.2 atm, P_{N_2} = 0.8 atm), and pure nitrogen (P_{Total} = 1 atm). As opposed to the high homogeneity of the oxygen-pyrolyzed films (see Figure 8a), decomposition in air and nitrogen led to inhomogeneous surfaces associated with the presence of Cu_2O microparticles, as confirmed by EDX analysis and in agreement with XRD (see Figure 7a).

(59) Gorbulev, V. A.; Fedorov, P. P.; Sobolev, B. P. *J. Less-Common Met.* **1980**, *76*, 55–62.

(60) Lange, F. F. *Science* **1996**, *273*, 903–909.

Scheme 2. Decomposition Chemical Reaction of the Metallic Trifluoroacetates in Air

$$Y(CF_3COO)_3\,(s) + 2Ba(CF_3COO)_2\,(s) + 3Cu(CF_3COO)_2(s) \xrightarrow{\text{air}}$$

$$\underbrace{YF_3\,(s) + 2BaF_2(s)} + (3-y)CuO\,(s) + y/2Cu_2O + 6CF_3COF\,(g) + 4COF_2(g) + (3-y/2)CO_2(g) + (7+y/2)CO(g)$$

$$BaF_2 + xYF_3 \longrightarrow Ba_{1-x}Y_xF_{2+x}$$

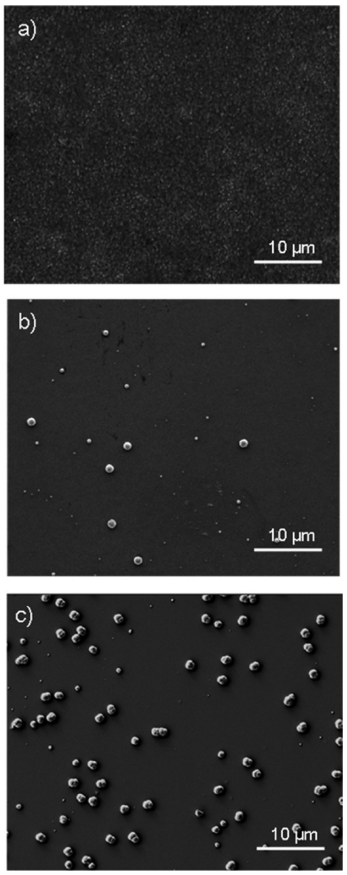

Figure 8. SEM images of as-decomposed films: (a) in oxygen, (b) in air, and (c) in nitrogen gas flow.

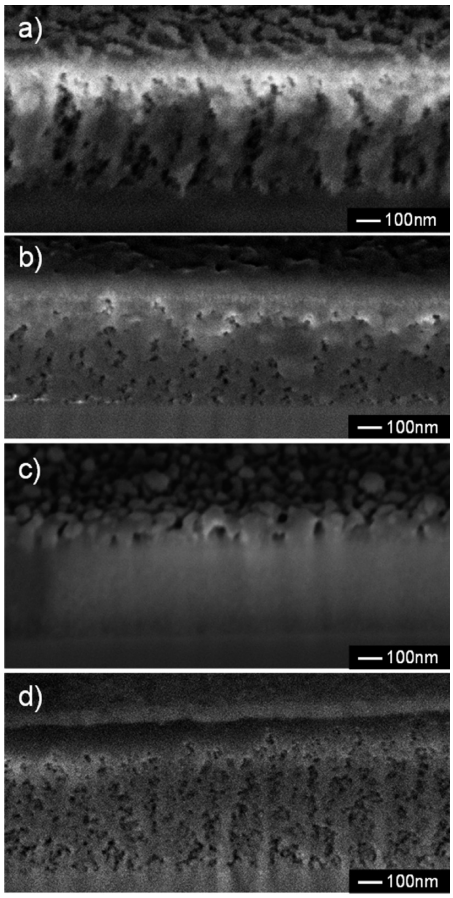

Figure 9. FIB images of pyrolyzed films processed at 310 °C in (a) pure oxygen, (b) in air, and (c) in pure nitrogen, as well as (d) those processed at 275 °C under a pure oxygen atmosphere.

Nevertheless, the presence of Cu_2O microparticles at the film surface of the pyrolyzed films is accompanied by a strong decrease in porosity, as can be observed in Figure 9. The FIB cross section of a standard-oxygen-pyrolyzed film (Figure 9a) evidences the formation of vertical open porosity which, because of its morphology and taking into account the poor mechanical properties of the films at this stage,[20] we attribute to fast gas escape toward the film surface. Through image analysis, we have estimated that oxygen-pyrolyzed films exhibit ~30% porosity. We would like to underline that the observed pores are not the commonly featured by chemically derived films in which shrinkage is the main source of porosity.[60] In our case, the vertical morphology of the pores leaves no room for doubt that the gas escape plays an important role in the formation of such pores. Therefore, porosity can be reduced by lowering the decomposition kinetics (i.e., lower pyrolysis temperature). Specifically, porosity has been reduced to ~15% in samples pyrolyzed at 275 °C instead of at 310 °C (see Figure 9d). In addition, the high exothermicity that is typical of thermo-oxidative decompositions also plays an important role in the porosity generation because the reaction results in a thermal runaway (self-heating), accelerating the gas flow toward the surface. Consequently, when the decomposition was conducted in less-oxidizing atmospheres (i.e., at low oxygen partial pressure), porosity decreased to ~5% in air, becoming negligible in N_2 (see Figures 9b and 9c). We attribute this observation to the fact that the enthalpy change becomes less negative, even becoming positive under inert atmospheres.[61,62]

We conclude that the porosity in pyrolyzed films can be accurately controlled by changing the decomposition reaction path, which is dependent on an intricate contribution of thermodynamic and kinetic factors determining the slow decomposition rate (gas escape rate) and the

(61) Yoshimura, Y.; Ohara, K. *J. Alloys Compd.* **2006**, *408*, 573–576.
(62) Mansour, S. A. A. *J. Therm. Anal.* **1996**, *46*, 263–274.

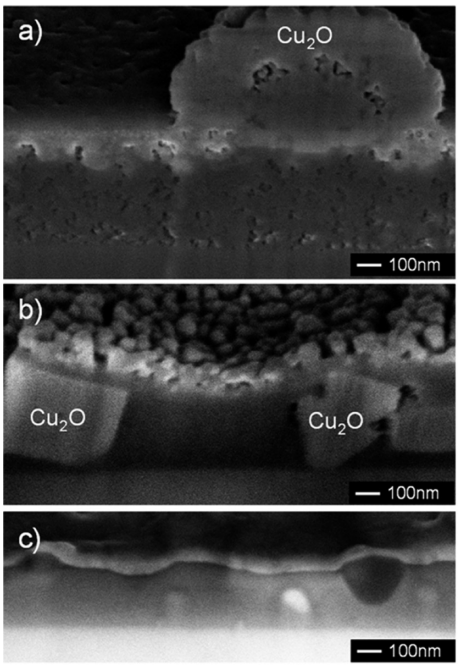

Figure 10. FIB cross-sectional images showing both Cu_2O coarsening and porosity reduction in pyrolyzed films processed (a) in air and (b) in an nitrogen atmosphere. (c) Unidentified particles in a grown YBCO film (from N_2 pyrolysis).

occurrence of a self-heating effect. Another relevant aspect of this study is that porosity is not dependent on the gas exhaust composition. Dense films with no blistering or bubbling are obtained with no need of reducing the fluorine content from the metal-organic precursors, as proposed for some authors.[31,32]

We have demonstrated that porosity is strongly reduced under less-oxidizing atmospheres; however, undesirable Cu_2O coarsening and further exodiffusion to the film surface then has been observed (see Figures 10a and 10b). The lower decomposition temperature of $Cu(TFA)_2$, with respect to the other salts, as well as slower decomposition when the P_{O_2} is reduced (see Figure 7b) seems to be the reason for Cu_2O ripening.[63] [Note: The decomposition temperature of each TFA salt has been investigated by TGA in air atmosphere: $T \approx 225$ °C for $Cu(TFA)_2$ and $T \approx 275-305$ °C for $Y(TFA)_3$ and $Ba(TFA)_2$.]

As stated in the Introduction, nonporous YBCO films are desired because pores behave as current blocking defects, thus decreasing the value of J_c.[37] However, it is not possible at the present stage to correlate the low porosity of films pyrolyzed in air and N_2 with the observed J_c values quantitatively, because a full investigation of the influence of YBCO growth conditions on the final microstructure in both cases should be performed. This study is beyond the scope of the present work; however, the typical J_c values of films pyrolyzed at low oxygen pressures and grown under standard conditions[17,20] were in the range of 2−3 MA/cm^2 at 77 K (see Figure 11), thus denoting that high-quality films also can be achieved under these pyrolysis conditions. Further investigation to optimize the growth process of TFA-YBCO films pyrolyzed at low oxygen pressures is currently underway.

(63) Araki, T. *Bull. Chem. Soc. Jpn.* **2004**, *77*, 1051–1061.

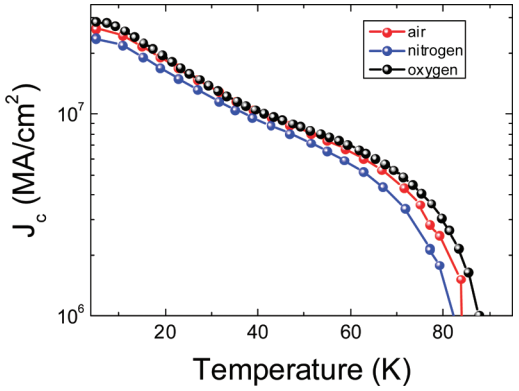

Figure 11. Temperature dependence of the critical current density of films decomposed in oxygen, air, and nitrogen.

Conclusions

The identification of the released gases during the metal-trifluoroacetate thermal decomposition in air has allowed us to determine the complete decomposition reaction, which, moreover, is valid at different atmospheres by varying the CO/CO_2 ratio in the released gases and the CuO/CuO_2 ratio in the solid product. Although the presence of HF in the gaseous phases was widely established, HF was not detected in the present study. Instead, CF_3COOH, CF_3COF, and COF_2 were released as fluorinated compounds. Note that the absence of HF in the gas exhaust is advantageous for the production of large-scale coated conductors from both technical (reactivity with SiO_2) and toxicity viewpoints.

Films pyrolyzed in a highly oxidizing atmosphere (such as pure oxygen) showed strong vertical porosity, because of the fast thermo-oxidative decomposition kinetics, together with a thermal runaway effect. Therefore, to avoid the formation of such pores, which are undesirable for the final superconducting performances, accurate control of both thermodynamic and kinetic effects of the decomposition reaction is needed. However, we have found new process conditions to eliminate the porosity in these materials. The gas exhaust rate is a key factor to control the residual porosity, being strongly reduced by lowering the gas flow oxygen partial pressure (i.e., air atmosphere). Accordingly, dense films were obtained after TFA decomposition in an inert atmosphere (i.e., nitrogen), because of the contribution of both lower decomposition kinetics and the endothermic nature of the reaction. In that case, however, Cu_2O coarsening and consequent phase segregation in the final YBCO superconducting film was observed.

Acknowledgment. We acknowledge the financial support from MICINN (MAT2008-01022, MAT2005-02047, MAT2006-26543-E, NAN2004-09133-CO3-01, Consolider NANOSELECT), Generalitat de Catalunya (Catalan Pla de Recerca SGR-0029 and XaRMAE), CSIC (PIF-CANNAMUS), and EU (HIPERCHEM, NMP4-CT2005-516858 and NESPA).